Novelty Journals

ISSN 2394-9651

International Journal of Novel Research in Physics Chemistry & Mathematics
Vol. 10, Issue 3, pp: (124-132), Month: September - December 2023, Available at: www.noveltyjournals.com

NONLINEAR OPTICAL AND LASER BREAKAGE EXPLORATION FOR PHOTONIC AND BIOLOGICAL APPLICATIONS

[1]Dr. G. KRISHNAVENI, [2]Dr. U. RIZWAN SULTHANA,
[3]Mr. S. S. SARAVANAKUMAR, [4]Dr. A.MAHENDRAPRABU

[1]Research Scholar, Department of Chemistry, Bharathidasan University, Tiruchirappalli-620023, Tamilnadu India.

[2]Assistant Professor, Department of Chemistry, M. S. S. Wakf Board College, Madurai-625020, Tamilnadu India.

[3]Guest Lecturer, Department of Physics, Sethupathy Government Arts College, Ramanathapuram-623502, Tamilnadu India.

[4]Guest Lecturer, Department of Physics, Government Arts College, Paramakudi-623701, Ramanathapuram District, Tamilnadu India.

[1] corresponding author, [2] co-corresponding author

DOI: https://doi.org/10.5281/zenodo.10184116

Published Date: 22-November-2023

Abstract: **The semi-organic single crystals of L-Glutamic acid hydrochloride a nonlinear optical material have been grown by an evaporation technique. The Powder Xray diffraction and FT-IR analysis showed the formation of semi-organic single crystals of L-Glutamic acid hydrochloride. The UV VIS absorption spectroscopic analysis and Tauc's plot confirmed that an optical quality and bandgap value of the crystals. The laser breakage threshold and micro-hardness properties of LGHCl single crystals were evaluated. The dielectric behaviour of LGHCl single crystal as a function of temperature was examined (300–350 K). The crystal's photoconductive properties were investigated in order to determine its photocurrent and dark current responses. The obtained results point out that the molecule is thermodynamically and optically stable, with a hyperpolarizability that is an equivalent to other molecules in its class.**

Keywords: **semi-organic single crystals of L-Glutamic acid, XRD, Nonlinear Optics, Laser breakage threshold, Photoconductivity.**

1. INTRODUCTION

Optoelectronics, telecommunications, and the laser industry have all greatly benefitted from the use of second- and third-order nonlinear optical materials [1-3]. It has become essential for technological advancements in recent years to find NLO materials with substantial second and third-order optical nonlinearities and quick reaction times. Because of their high damage threshold, wide transparency range, lower UV cutoff wavelength, high nonlinear coefficient, high mechanical stability, and high thermal stability, semi-organic materials combine the enhanced properties of organic and inorganic crystals. Due to their dipolar nature, NLO applications can take use of their unique physical and chemical features [4]. Second harmonic generation (SHG) is one of the most exciting phenomena observed in most crystals without a symmetry centre and is used for frequency conversion, optical modulation, etc.

Due to their high SHG efficiency and laser damage threshold (LDT) values, Lithium niobate and others are employed for NLO applications [5- 7]. However, creating defect-free crystals from the above components is arduous. Thus, photonic applications require a material with excellent NLO properties and easy single crystal formation. All amino acids except glycine have chiral carbon atoms and noncentrosymmetric crystal structures, making them good candidates for second harmonic and coherent blue-green laser generation [8, 9]. These crystals have SHG efficiency comparable to the aforementioned materials and can be formed utilizing slow evaporation solution growth (SESG) without melt growth methods.

Molecular engineering and chemical synthesis allow amino acids to be modified and optimized [10]. In this present work, slow evaporation solution growth method was used to harvest 80 single crystal of L-Glutamic acid hydrochloride.

Experimental

Synthesis and crystal growth of L-Glutamic acid hydrochloride

L-Glutamic acid was dissolved in deionized water and grew in an equimolar ratio with hydrochloric acid to form a single crystal of LGHCl.

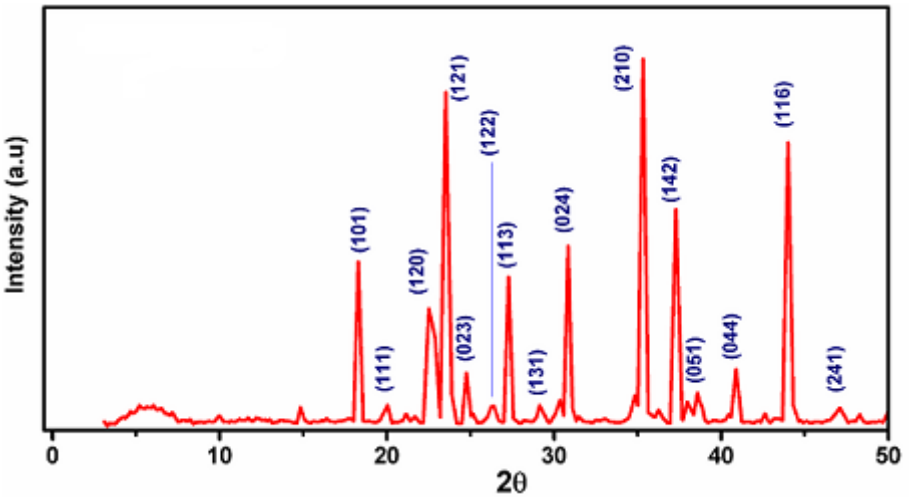

Figure 1: XRD pattern of LGHCl

On the basis of the solubility data [11], it was decided to create a super saturation solution and stir it for two hours. After being filtered and allowed to evaporate at room temperature, the solution was discarded. Using the slow evaporation solution growth method, optically transparent single crystals were grown in 25 days due to spontaneous nucleation. The technique of recrystallization improved the quality and size of the crystal. Figure 1 depicts the Bravais-Friedal-Harker (BFDH) morphology of the crystal of LGHCl crystal.

Characterization Techniques

X-ray diffraction investigation was performed on the generated LGHCl crystal using a Bruker AXS Advance X-ray diffractometer. The reference crystal was CuKα (=1.5406109 Å), and the data was recorded. The FT-IR spectrum of the material was obtained using a Perkin Elmer spectrometer using the KBr Pellet technique in the range of 4000-400 cm^{-1}. The UV-Vis absorption analysis of the material was performed with a Shimadzu UV-Vis spectrometer in water solution in the spectral range of 187-1200 nm. The Kurtz and Perry powder approach was used to test the second harmonic generation efficiency of LGHCl. For this experiment, the Q switched Nd:YAG laser of 1064 nm wavelength was used as the optical source. The powder samples were carefully crushed to a particle size of 125-150 µm, and then they were loaded in a capillary tube with a diameter of around 1.5 mm. The power metre was used to determine the amount of input energy, and it came out to be 6 mJ/pulse. The laser employed used to have 1064 nm wavelength, 8 ns pulse with, as well as 10 Hz repetition rate, and it was focused on the sample. The sample causes a green light emission at 532 nm, which is picked up with the aid of photomultiplier tube. The signal is first received by a photomultiplier tube, which transforms it into an electrical signal. With the aid of Q-switched Nd: YAG laser, the laser induced damage threshold (LDT) of LGHCl

Novelty Journals

ISSN 2394-9651

International Journal of Novel Research in Physics Chemistry & Mathematics
Vol. 10, Issue 3, pp: (124-132), Month: September - December 2023, Available at: www.noveltyjournals.com

was determined. Using a Hioki 3532-50 LCR metre, a dielectric investigation was conducted in the frequency range of 50 Hz to 5 MHz at temperatures between 300 and 400 K. Utilizing Keithley-6517 B electrometer, the photoconductivity of an LGHCl crystal was measured. Under 100 mW/cm^2 of radiation, the photocurrent (IP) was measured for an applied voltage range of 1–15 V. The measured sample's volume and surface area are 0.73 cm^3 and 5.823 cm^2, respectively. Variable loads of 10g to 100g were used to create indentations on the surface of the grown crystal, which was placed correctly on the microscope's base. Five impressions were made for each weight, and the optical microscope was used to determine the average pattern of diagonal lengths of the imprints.

2. RESULT AND DISCUSSION

X-ray diffraction analysis

The single crystal, fine powder of LGHCl was scanned in the 2θ range of 3° to 80°. Figure 1 depicts the powder XRD pattern that was recorded. The emergence of quite sharp and strong diffraction peaks demonstrated that LGHCl was crystalline and free from structural grain boundaries [12]. LGHCl crystal XRD [38] indicates that it is an orthorhombic system with the P212121 space group. The dimensions of the cell are a=5.1016(1) A°, b=11.6386(4) A°, and c=13.2500(3) A°. This is consistent with the previously reported figure [13].

Optimized geometry

The experimental data and computed optimized structural parameters of LGHCl were both taken from the Gaussian'09 programme package using the B3LYP/6-311++G(d,p) level of theory and X-ray diffraction data [13] and the calculated geometric parameters are most likely caused by the interactions between molecules in the crystalline state. The difference could be explained by the fact that the calculations were done on a single molecule in the gaseous phase. In contrast to what was found in experiments, when many molecules are packed together, this is called the condensed phase.

Most of the optimized bond lengths are close to the experimental values. This is because molecules interact with each other. The N-H bonds with lengths of 1.084 Å, 1.0038 Å, and 1.006 Å, respectively. The NH...Cl and N-H...O intramolecular hydrogen bonds are what make the N8-H9 and N8-H11 bonds longer. The distance between Cl-H and O-H was found to be 1.821 and 2.191, which is much smaller than van darwaal's radii of 2.95 and 2.72. This suggests that N8-H9...Cl1 and N8-H11...O4 could form intramolecular hydrogen bonds. Due to the presence of electronegative Cl and O atoms, the hydrogen atoms next to each other in the NH^{3+} group, such as H9 and H11 and H10 and H11, move closer to each other. This makes the angles of the H-N-H bonds smaller than the angles of the H9-N8-H10 bonds.

Vibrational spectral analysis

The experimental FT-IR spectrum of the title compound is shown in Figure 2. The asymmetric stretching vibrations of NH_2 and the symmetric stretching vibrations of NH_2 are typically detected in the area 3380-3350 cm^{-1} and 3310-3280 cm^{-1}, respectively [14].

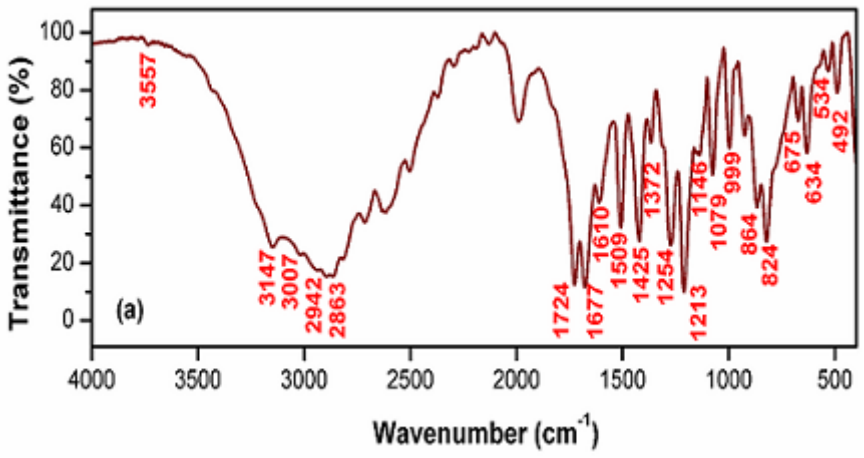

Figure 2: FTIR spectrum of LGHCl

In amino acid derivatives, the protonation of the NH^{3+} group can cause a band position shift toward the region of 3300-3100 cm^{-1} and 3100-2600 cm^{-1}, respectively, for asymmetric and symmetric NH^{3+} stretching [15-19]. In the infrared spectrum, the stretching vibration bands caused by NH^{3+} appear to be wider and less intense than those caused by unmodified NH_2 groups. In the infrared spectrum, the asymmetric stretching mode of the NH^{3+} group can be seen at a frequency of 3147 cm^{-1} as a faint and broadband signal. In addition, the position, broadness, and wavenumber of the NH^{3+} asymmetric stretching mode of vibration point to the formation of a powerful N-H...Cl intra-molecular hydrogen bonding between the NH^{3+} group and the Cl^- ion. This is indicated by the fact that the mode of vibration has a lower wavenumber.

Carboxylic acid, OH stretching has several bands in the 3700-3300 cm^{-1} region, depending on their degree of association, and the fundamental stretching vibrations of the hydroxyl group of monomers, combination, and overtone bands are commonly expected in the 3570 cm^{-1} region [20]. In the IR spectra of LGHCl, OH stretching vibration of carboxylic group is detected as a faint band at 3557 cm^{-1}. The C=O group of saturated aliphatic carboxylic acid absorbs considerably between 1755 and 1700 cm^{-1} [20] in amino acids. The medium-intensity band found at 1724 cm^{-1} in both IR spectra corresponds to the C=O stretching mode of vibration. The typical zone for O-H deformation vibrations in the plane is 1400 to 1200 cm^{-1}. The bands of medium intensity found in the infrared at 1254 cm^{-1} correspond to the C-O-H in-plane bending modes of vibration. The usual zone for O-H out-of plane bending vibrations of carboxylic groups is 700-600 cm^{-1} [20, 22-29]. Medium and strong bands are seen at 675 cm^{-1} and 634 cm^{-1} in the IR spectrum. C-O stretching modes for amino acid hydro halides are often observed between 1230 and 1215 cm^{-1} [20]. Strong band seen in the IR spectra at 1213 cm^{-1}, ascribed to CO stretching vibration.

The CH_2 scissoring deformation vibration, which is approximately 1463 cm^{-1} [30, 31] is decreased to around 1440 cm^{-1}. A carbonyl, nitrile, or nitro group decreases the adjacent CH_2 group's frequency to around 1425 cm^{-1} and its intensity by about [28-31]. At 1425 cm^{-1}, the CH_2 scissoring vibrations appear as a band of moderate intensity in the IR spectra. Rocking, wagging, and twisting vibrations appear in the area of 1422-719 cm^{-1} for the CH_2 group bending vibration [30-33]. The medium to faint CH_2 wagging vibration is noticed in the IR band at 1372 cm^{-1}. C-H stretching vibrations have often appeared between 3000 and 2850 cm^{-1} for amino acids [20]. In the IR spectra of LGHCl, the C-H stretching modes are detected as a weak and broad band at 2942 cm^{-1}.

Optical absorption spectra

UV-Visible absorption spectra played a crucial role for NLO materials, as nonlinear optical materials can only be used practically if they have high transparency in the ultraviolet, visible, and near-infrared regions. It is obvious from the UV-Vis spectra that the reported cut-off wavelength of LGHCl is 192 nm.

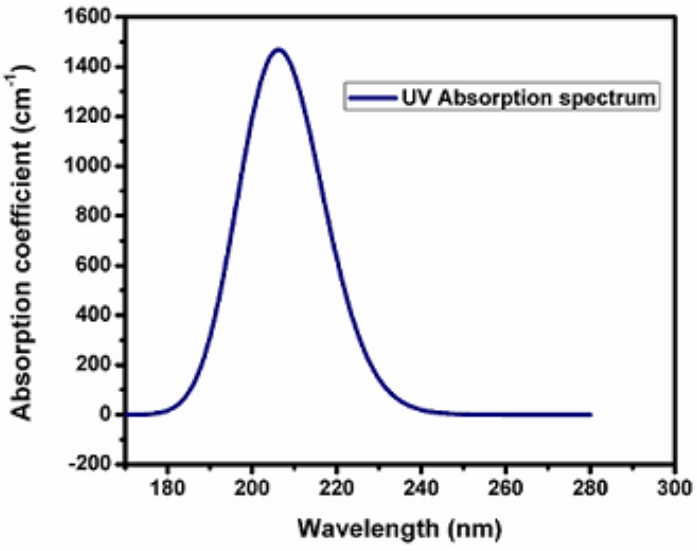

Figure 3a: Optical absorption spectrum of LGHCl

The experimental spectra reveal that LGHCl is transparent throughout the full 237-1200 nm wavelength range, with no absorption peaks. This result implies that LGHCl crystal is suited in blue-violet region for NLO, optoelectronic, and other applications.

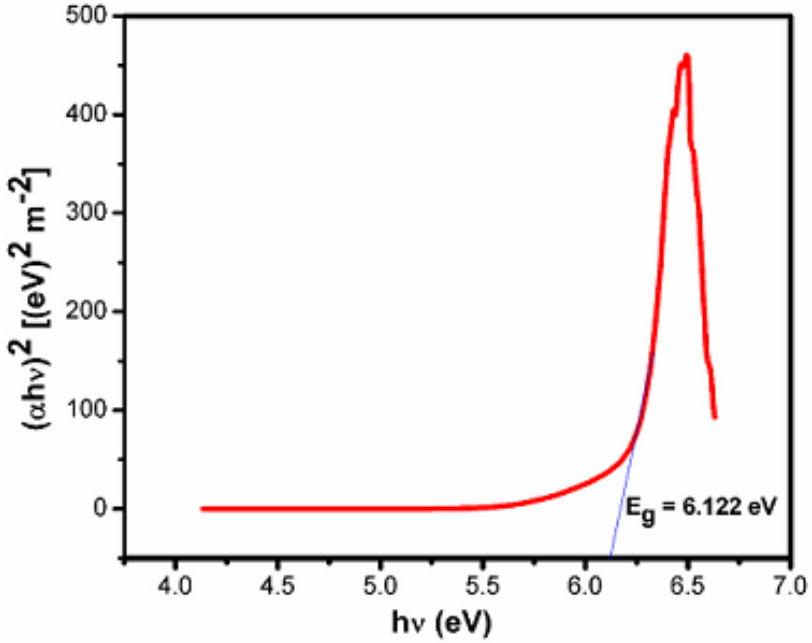

Figure 3b: Tauc's plot of LGHCl

Second Harmonic generation

The SHG efficiency ofLGHClis measured using Kurtz and Perry powder technique.

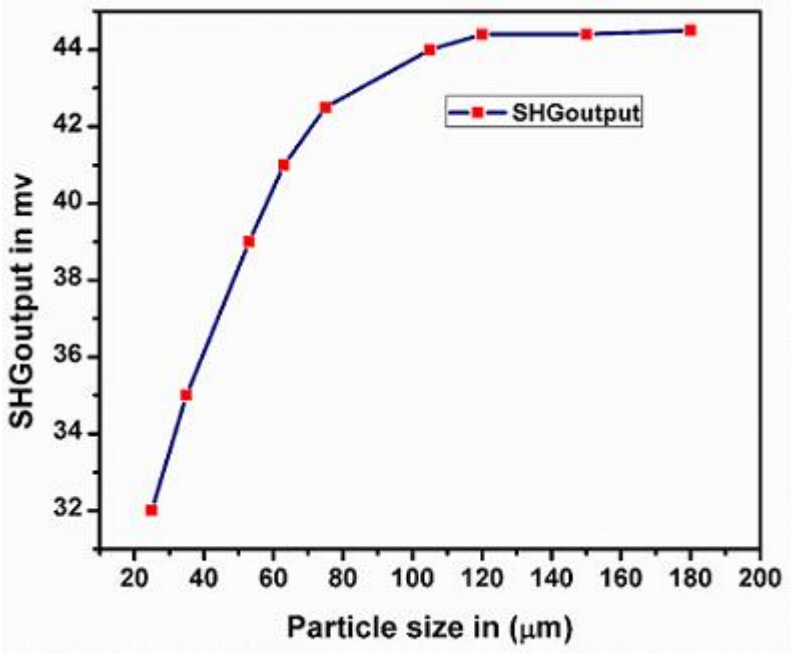

Figure 4: SHG output (mV) Vs Particle Size (µm)

The SHG efficiency was measured and compared with standard KDP. The SHG signals of 44 mV and 27 mV were obtained for LGHCl and KDP, respectively. From the Figure 4, it can be concluded that the relative SHG efficiency of LGHCl is 0.67 times greater than that of standard reference KDP crystal.

Novelty Journals

ISSN 2394-9651

International Journal of Novel Research in Physics Chemistry & Mathematics
Vol. 10, Issue 3, pp: (124-132), Month: September - December 2023, Available at: www.noveltyjournals.com

Laser breakage Threshold (LDT) study

The potential of the single crystal to resist damage caused by the laser is vital because it lets them be used in optical applications. In general, the LDT value for a single shot is significantly greater than the LDT value for multiple shots [34].

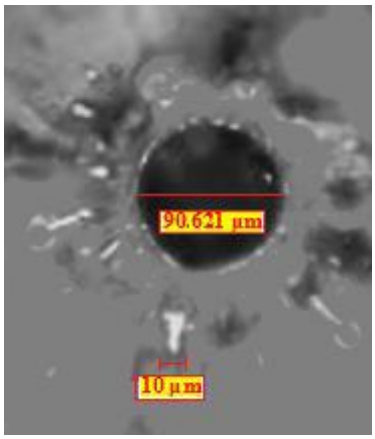

Figure 5: Microscopic image of single shot laser induced damage pattern along (1 0 1) plane

The superior optical quality LGHCl crystal was chosen and checked with an optical microscope. The crystal was then put on the goniometer so that the laser could shine on its (1 0 1) plane. The attenuator controlled how much energy came out and made sure that it went to the crystal.

Compound	**Laser Damage Threshold (GW/Cm^2)**
Potassium dihydrogen Phosphate	0.2
Urea	1.5
Benzimidazole	2.9
L-Arginine Bis(trifluoroacetate)(LATBF)	0.79
L-Glutamic acid Hydrochloride	3.2

The damaged part of micrograph of the LGHCl single crystal along the (10 1) plane (shown in Figure 5) shows that there are a few blobs around the damaged area. This is because the area melted and then solidified again.

The relationship [34] was used to figure out the LDT value of LGHCl.

$I = E/\tau\pi r^2$…. (7)

3.29 GW/cm^2 was the amount of laser damage power density found in LGHCl. This LDT value was also compared with some organic and semiorganic crystals (Table), such as Potassium dihydrogen phosphate (0.2 GW/cm^2) [35], Urea crystals (1.5 GW/cm^2) [35], Benzimidazole (2.9 GW/cm^2), and L-Arginine Bis(trifluoroacetate)(LATBF) (0.79 GW/cm^2) [35]. So, the results depicted that LGHCl has a higher laser damage threshold than most of the otherinorganic and organic crystals shown in below Table.

Parameters	**B3LYP/C6- 311++G(d,p)**
HOMO energy, EHOMO (eV)	-7.3371
LUMO energy, ELUMO (eV)	-0.7434
HOMO- LUMO energy gap, ΔEGAP (eV)	6.5936
Ionisation potential, IP (eV)	7.3371
Chemical potential, μ (eV)	-4.0403

Photoconductivity study

The variation of field dependent dark current (Id) and photocurrent (Ip) measurements of the LGHCl crystal was carried out by a two probe technique at room temperature. The sample was shielded from radiation and the applied voltage rose from 1 V to 10 V in 1 V steps for dark current measurements. A 100 W halogen lamp with iodine vapor and tungsten

filament illuminated photocurrent measurements. Field dependence of dark current and photocurrent of LGHCl crystals is depicted in Figure 6. Clearly, the dark and photocurrent levels both grow linearly with the voltage level, but the photocurrent is comparatively smaller than the dark current value, which is known as negative photoconductivity. A two stage approach is supposed to explain negative photoconductivity in accordance with the Stockmann model. The lower energy level features a capture cross section for electrons from the conduction band and holes from the valance band. Presence of radiation, electron-hole recombination takes place and reduction of the number of mobile charge carriers exhibit the negative photoconductivity. [18] At ambient temperature, a fluctuation in the field dependent dark current (Id) and photocurrent (Ip) measurements of the LGHCl crystal was measured using a two-probe approach. In order to measure the dark current, the sample was shielded from any type of radiation sources, and also the supplied voltage was incrementally increased insteps from 1 - 10 V range. For the purposes of photocurrent measurements, illumination was provided using a 100 W halogen lamp with a tungsten filament and iodine vapour contained within the bulb. The relationship between the field, dark and photocurrent values of LGHCl crystals is depicted in Figure 6.

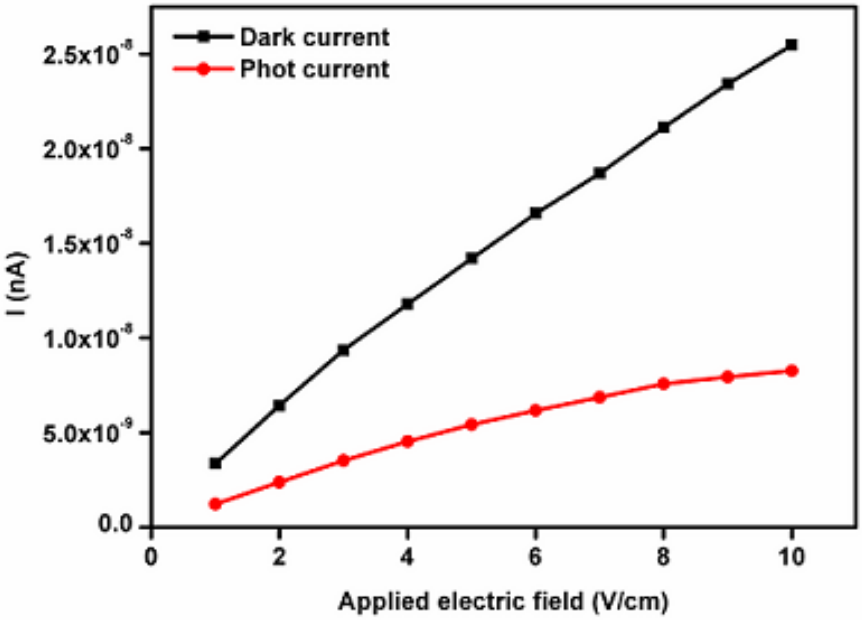

Figure 6 Photocurrent and dark current response of LGHCL with applied electric field

The energy level with the larger value can be found in the region between the Fermi level and the conduction band. The energy level with the lower value can be found in the region near to the valence band. The lower energy level features a capture cross section for electrons from the conduction band and holes from the valance band. In the presence of radiation, electron-hole recombination takes occur, which results in a decrease in the total number of mobile charge carriers, which demonstrates the negative photoconductivity effect [18].

3. CONCLUSION

Using the slow solvent evaporation method, a semi-organic LGHCl single crystal has been produced. Powder X-ray diffraction (P-XRD) analysis validated the crystalline property of generated crystal. FT-IR spectroscopic technique have been used to examine the molecular vibrations of crystals of LGHCl. Using UV–vis absorption measurements, the range of optical transmission was determined; a peak was seen at 192 nm as the UV cutoff wavelength, and the band gap energy was also computed. The Second Harmonic Generation conversion efficiency of LGHCl is 1.62 times that of KDP crystal, the industry standard and the compound exhibits its phase matching behavior. The values of the HOMO and LUMO energy gaps reflect the likelihood of charge transfer within the molecule. The first and second order hyper polarizability are estimated at the B3LYP/6-311++G(d,p) level of theory. Thus, the aforementioned tests demonstrated that LGHCL could be a promising material for Second and third harmonic generation NLO applications as well as biological applications.

REFERENCES

[1] H. O. Marcy, L. F. Warren, M. S. Webb, C. A. Ebbers, S. P. Velsko, G. C. Kennedy, G. C. Catella, Appl. Opt. 31 (1992) 5051.

[2] X. Q. Wang, D. Xu, D. R. Yuan, Y. P. Tian, W. T. Yu, S. Y. Sun, Z. H. Yang, Q. Fang, M. K. Lu, Y. X. Yan, F. Q. Meng, S. Y. Guo, G. H. Zhang, M. H. Jiang. Mater. Res. Bull. 1999, 34, 2003.

[3] Sutherland R. L. Handbook of nonlinear optics. 2nd ed. NewYork: Dekker; 1996.

[4] B.A. Fuchs, K. Chai syn, P. Stephan Velsko, Appl. Opt. 28 (1989) 4465–4472.

[5] D.W. Chen and J.J. Yeh, Opt.Lett., 1988, 13(10), 808-810.

[6] G.D. Boyd, R.C. Miller, K. Nassau, W.L. Bond and A. Savage, Appl. Phys. Lett., 1964, 5(11), 234-236.

[7] C. Chen, Y. Wu, A. Jiang, B. Wu, G. You, R. Li and S. Lin, J. Opt.Soc. Am. B., 1989, 6(4), 616-621.

[8] G. R. Kumar, S. G. Raj, R. Mohan, and R. Jayavel, Cryst. Growth Des., 2006, 6(6), 1308-1310.

[9] S. Suresh, A. Ramanand, D. Jayaraman and P. Mani, Rev. Adv.Mater.Sci., 2012, 30, 175–183.

[10] G. Dematos, V. Venkataraman, E. Nogueria, M. Belsley, P.A Criado, M.J. Dianez and E.P. Garrido, Synth. Met., 2000, 115, 225-228.

[11] David L. Bryce, Gregory D. Sward, and Samyuktha Adiga, J. AM. CHEM. SOC. 2006, 128, 2121-2134

[12] M. Senthil Pandian, K. Boopathi, P. Ramasamy, G. Bhagavannarayana, Mater. Res. Bull. 47 (2012) 826–835.

[13] Yi Jian Zhang,a Zhan Shu,b Wei Xu,b Gang Chenb and Zu-Guang Lic, Acta Cryst. (2008). E64, o446.

[14] D.L. Vein, N.B. Colthup, W.G. Fateley, J.G. Grasselli, The Handbook of Infrared and Raman Characteristic Frequencies of Organic Molecules, Academic Press, New York, 1991.

[15] J. Baran, A.J. Barnes, H. Ratajczak, Spectrochim. Acta 51A (1995) 197–214.

[16] A. Novak, Struct. Bonding 18 (1973) 177–216.

[17] T. Edsall, H. Scheinberg, J. Chem. Phys. 8 (1940) 520–525.

[18] M. Narayana Bhat, S.M. Dharmaprakash, J. Cryst. Growth 236 (2002) 376–380.

[19] L.J. Bellamy, The Infrared Spectra of Complex Molecules, Chapman and Hall, London, 1980.

[20] G. Socrates, Infrared and Raman Characteristic Group Frequencies, John Wiley & Sons, West London, UK, 2001.

[21] D. Lin-Vien, N.B. Colthup, W.G. Fateley, J.G. Graselli, The Hand Book of Infrared and Raman Characteristic Frequencies of Organic Molecules, Academic Press, New York, 1991.

[22] S. George, Infrared and Raman Characteristic Group Wavenumbers, Tables and Charts, third ed., Wiley, Chichester, UK, 2001.

[23] C. Ravikumar, I. Hubert Joe, V.S. Jayakumar, Chem. Phys. Lett. 460 (2008) 552–558.

[24] C. Ravikumar, I. Hubert Joe, D. Sajan, Chem. Phys. 369 (2010) 1–7.

[25] N.P.G. Roeges, A Guide to the Complete Interpretation of Infrared spectra of Organic Structure, Wiley, New York, 1999.

[26] G. Treboux, D. Maynau, J.P. Malreu, J. Phys. Chem. 99 (1995) 6417–6423.

[27] S. E. Wiberley, S. C. Bunce, and W^. H. Bauer, Anal. Chem. 32, 217 (1960).

[28] R. D. Hill and G. D. Meakins, / . Chem. Soc, London p. 760 (1958).

[29] W. B. Wright, Jr., / . Org. Chem. 24, 1362 (1959).

[30] N. B. Colthup, L. H. Daly, S. E. Wiberley, Introduction to Infrared and Raman Spectroscopy, Academic press, Inc, London, 1975.

[31] C. L. McMurry and V. Thornton, Anal. Chem. 24, 318 (1952).

[32] N. B. Colthup, / . Opt. Soc. Amer. 40, 397 (1950).

[33] J. Binoy, J. P. Abraham, I. Hubert Joe, V. S. Jayakumar, G. R. Pettit, O. F. Nielsen, J. Raman Spectrosc. 2004, 35, 939.

[34] M. Krishnakumar, S. Karthick, K. Thirupugalmani, S. Brahadeeswaran, Opt. Mater. 66 (2017) 79–93.

[35] Anuj Krishna, N. Vijayan, Shashikant 655 Gupta,cKanika Thukral, V. Jayaramakrishnan, Budhendra Singh, J. Philip,f Subhasis Das, K. K. Maurya G. Bhagavannarayana, RSC Adv., 4 (2014) 56188.

[36] R.H. Bube, Photoconductivity of Solids, Wiley Interscience, New York, 1981.

Statements & Declarations

We confirm that the manuscript has been read and approved by all named authors and that there are no other persons who satisfied the criteria for authorship but are not listed. We further confirm that the order of authors listed in the manuscript has been approved by all of us.

Data Availability Statement

The authors confirm that the data supporting the findings of this study are available within the article.